Rock magnetism in two loess–paleosol sequences in Córdoba, Argentina

S. Rouzaut, M. J. Orgeira, C. Vásquez, R. Ayala, G. L. Argüello, A. Tauber, R. Tófalo, L. Mansilla & J. Sanabria

Environmental Earth Sciences

ISSN 1866-6280

Environ Earth Sci
DOI 10.1007/s12665-014-3855-8

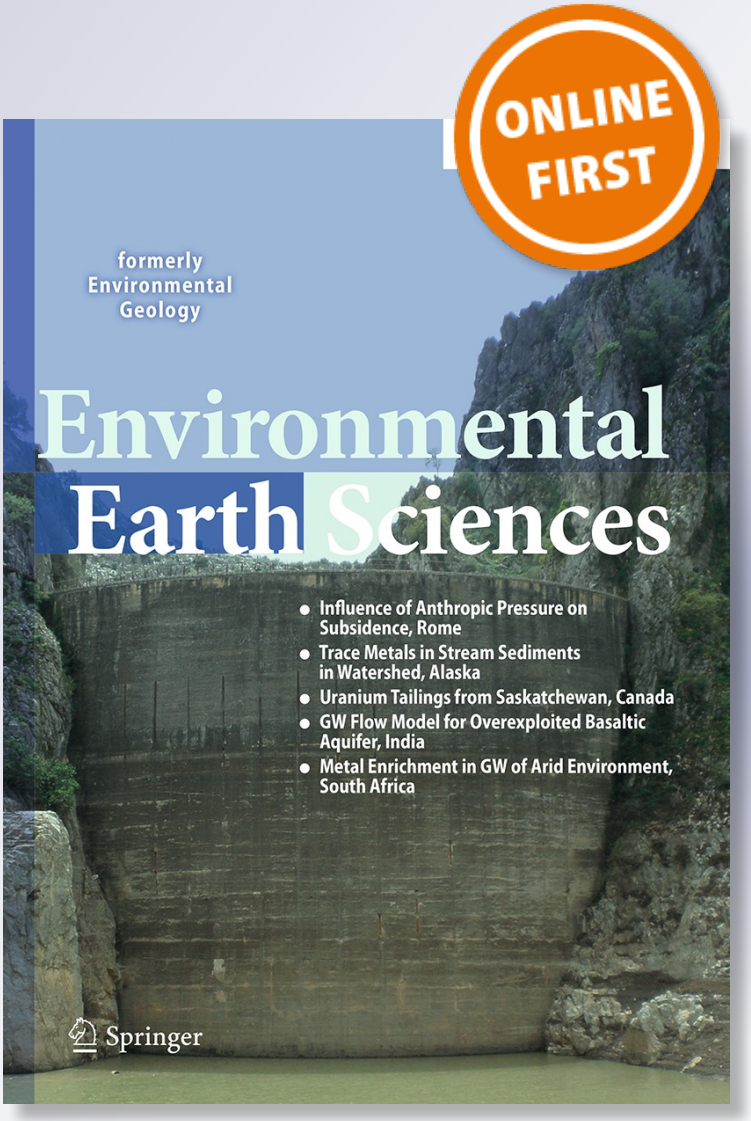

Springer

Environ Earth Sci
DOI 10.1007/s12665-014-3855-8

ORIGINAL ARTICLE

Rock magnetism in two loess–paleosol sequences in Córdoba, Argentina

S. Rouzaut · M. J. Orgeira · C. Vásquez · R. Ayala · G. L. Argüello · A. Tauber · R. Tófalo · L. Mansilla · J. Sanabria

Received: 26 January 2014 / Accepted: 3 November 2014

Abstract This work presents new rock magnetic results along two loess–paleosol profiles in nearby locations in Argentina. The main objective of this study is to compare the magnetic signals and mineral content of two profiles and determine if the climate during Marine Isotope Stage 5 (MIS 5) and MIS 3 were similar to the present one. The two profiles are located in two different geomorphological settings, with effects on the water saturation characteristics and seasonality. Selected samples taken at these profiles were analyzed using laboratory procedures and environmental magnetism parameters to determine the climatic influence during the Late Pleistocene. Despite their proximity there are several differences between both profiles, such as their depth and geomorphological positions among others. The results of these analyses led to the following conclusions: climate conditions during MIS 5 were very similar to those of the present conditions. The hypothesis for this area suggests a slight increase in the magnetic signal associated with the generation of small amounts of magnetite and preservation of detrital magnetite and titanomagnetite. The results in this paper show a slight gain in the buried soils of Córdoba that would confirm the hypothesis.

Keywords Rock magnetism · MIS 5 · Mineralogy · Geomorphology

Introduction

Studies of environmental magnetism have obtained satisfactory results in the acquisition of paleoclimate data, mainly in the Loess Plateau of China (e.g., Banerjee and Hunt 1993; Heller et al. 1993; Maher and Thompson 1995; Liu et al. 1995; among others).

Loess and paleosol sequences have proved to be a good record of climate changes, since magnetic properties are an

S. Rouzaut (✉)
Becaria CONICET, Córdoba, Argentina
e-mail: srouzaut@gmail.com

S. Rouzaut · J. Sanabria
Cátedra de Pedología, Escuela de Geología, F.C.E.F.y N. UNC, Vélez Sarsfield 1611, CP 5016 Córdoba, Argentina

M. J. Orgeira · C. Vásquez
Dpto. Ciencias Geológicas, FCEN, UBA, IGEBA, Ciudad Universitaria Pab. II, Nuñez, Buenos Aires, Argentina

R. Ayala
Cátedra de Mineralogía e Industrias Extractivas, Métodos de Investigación Mineral y Laboratorio Vaquerías, UNC, Córdoba, Argentina

G. L. Argüello
Ejercicio libre de la profesión, Córdoba, Argentina

A. Tauber
Cátedra de Paleontología, Escuela de Geología, F.C.E.F.y N. UNC, Vélez Sarsfield 1611, CP 5016 Córdoba, Argentina

R. Tófalo
Dpto. Ciencias Geológicas, FCEN, UBA, IDEAN, Ciudad Universitaria – Pab. II, Buenos Aires, Argentina

L. Mansilla
Cátedra de Geomorfología, Escuela de Geología, F.C.E.F.y N. UNC, Vélez Sarsfield 1611, CP 5016 Córdoba, Argentina

Published online: 16 November 2014

excellent proxy to detect these shifts (Oches and Banerjee 1996; among others).

Currently, there are several hypotheses regarding the origin of the magnetic signal in paleosols developed on loess (Heller and Evans 1995; Maher 1998; Boyle et al. 2010), although none of them seem to be widely accepted. This study follows the model proposed by Orgeira et al. (2011), which attributes a mainly inorganic origin to the variations in magnetic mineralogy during pedogenesis. This model is based on Fe redox processes throughout successive seasonal stages (Orgeira and Compagnucci 2006). This hypothesis involves climate, rainfall and evapotranspiration as essential vectors for the development of soil profile, in addition to soil microclimate and texture, among other factors.

However, the climatic dependence of magnetic enhancement in loessial soils does not correlate with the climate record in Argentine sequences (Orgeira et al. 1998, 2002; Bidegain et al. 2001, 2005; Rouzaut et al. 2012). To explain these differences, Orgeira et al. (2011) developed a model which incorporated a broader set of climate parameters that influence the processes of formation–destruction of magnetic particles, thus achieving a successful modeling of the magnetic signal. However, in this quantitative model, the geomorphological differences were not taken into account, and this may have affected the diagenetic processes involved in the formation–destruction of the magnetic particles. To evaluate these effects, two profiles were studied in the province of Córdoba, Argentina.

The formation of pedogenic magnetite is conditioned by soil drainage, intermediate pH, the presence of organic matter and cation exchange capacity. Both the weathering of iron primary minerals and the neoformation of secondary minerals are affected by the pH–Eh ratio. Redox conditions are induced by oscillations in the water table, and lead to the dissolution of magnetite and the loss of secondary iron oxides.

The loss of magnetite would also be prompted by organic ligands present in the upper soil horizons and by water enriched in silica found within the pores. The idea of the existence of a pedogenetic threshold driven by water balance in the soil was used by Orgeira and Compagnucci (2006, 2010) to explain the increase and decrease of magnetic signal in the loessial soils of the world.

Orgeira et al. (2011) suggest a link between climate and magnetic signal, and formulated the W index or moisture ratio ($W = \mathrm{MAR}/P_{\mathrm{etc}}$), where W is the moisture ratio, P_{etc} is the monthly potential evapotranspiration corrected for latitude and month length and MAR is the mean annual rain.

The $W_0 \approx 1$ (W_0: saturated pores containing water available for evapotranspiration) index marks the transition between relatively dry and water saturated conditions. $W > W_0$ represents the beginning of a soil saturation regime, a decrease in the frequency of dry/wet cycles and the end of magnetite production. The condition $0.5 < W_0 < 1$ indicates poorly drained soils.

In this paper, the magnetic properties of two profiles located in the province of Córdoba are compared to establish paleoclimatic implications.

The main objective of this study is to compare the magnetic signals and mineral content of two profiles which contain the same geological units and which are close to each other but represent different geomorphological positions. It should be noticed that according to Orgeira et al. (2011), the rainfall and the current evapotranspiration of Córdoba are compensated (W close to zero), it means there is a balance between the generation of pedogenetic magnetite and the loss of magnetic particles of detritic origin should not be expected. Also, W close to zero means that the production of superparamagnetic magnetite and particles of maghemite that caused magnetic enrichment is almost compensated for destruction of magnetic minerals. During the climatic dry phase the magnetite surface oxidizes and a superficial crust of maghemite is formed; its growth is controlled by the diffusion of Fe II ions towards the exterior. If a particle of magnetite partially oxidized is exposed to reductive conditions during the humid cycle, the maghemite dissolves. The rate of destruction is proportional to the mass of maghemite, which depends on the average time between the rainy events and the frequency of the humid-dry cycles.

Location and geological context of the area

Loess deposits in Argentina are located in the central region of the country, in the so-called Llanura Pampeana, which includes the provinces of San Luis, Santa Fe, Córdoba, La Pampa and Buenos Aires (Frenguelli 1955; Teruggi 1957; Muhs and Zárate 2001; among others). These deposits are sequences of paleosols and loess which have been re-worked by water and are estimated to be from the Pleistocene–Late Holocene. The texture is a very homogeneous sandy clay loam, with a noticeable increase in the percentage of sand towards the SW (Zárate and Blasi 1993; Zárate and Tripaldi 2011).

Suggested source areas according to Iriondo and Kröhling (1995) are the flood plains and fluvial fans of the Bermejo, Salado and Desaguadero rivers which drain the Andean glaciers. A small portion of this material would have come from the Sierras Pampeanas of Córdoba and San Luis, and from volcanic emissions in the provinces of Mendoza and Neuquén (Iriondo 1990, 1997). Bloom (1990) proposes the Puna volcanoes as an alternative source, and Clapperton (1993) suggests the Bolivian Altiplano. Zárate (2003) mentions the Andes, Sierras

Pampeanas and the basin of the Paraná River. However, despite these differences, all of the above-mentioned authors agree that W and SW winds were responsible for transporting the material. In terms of minerals, the Pampean loess is mostly made up of traces of volcanic glass, plagioclase and quartz (Teruggi 1957; Muhs and Zárate 2001).

The studied profiles are in the Llanura Chacopampeana geological province, within the Llanura Pampeana subprovince, where two associations can be distinguished: the Depresión Periférica (peripheral depression) and the Plataforma Basculada (tilted platform), (Capitanelli 1979). The tilted platform consists of two subassociations (Sanabria et al. 2006): the Plataforma Basculada Ondulada and the Plataforma Basculada Plana (the undulated tilted platform and the flat tilted platform) (Fig. 1).

The Corralito I profile is located on the undulated tilted platform, which is made up of both long and rounded hills, with slopes ranging between 1 and 3 % and heights of around 10 m. They are usually affected by rill erosion, both rectilinear and meandering, and in some cases gullies can also develop. The topographic position of Corralito I in this subassociation causes a concentration of water flow since it is located on a drainage line, and as a consequence a greater horizonation in soil profiles can be expected (Porta Casanellas et al. 2003).

The Corralito II profile is located 6 km east from Corralito I in the flat tilted platform subassociation, which is characterized by gently undulating hills with slopes of around 1 %.

The parent material in both subassociations is re-transported loess, with an approximate age of between 115 and 5 ka (Frechen et al. 2009; Kemp et al. 2006). Thickness ranges from 4 to 20 m, and the sediments are homogeneous and friable, with 0.2–5 % of $CaCO_3$ content and 65–70 % of coarse silt.

The climate for both profiles is mesothermal with warm, humid summers and mild, dry winters. The average annual rainfall is 789 mm, with a maximum of 1,348 mm for the hydrological year 1978/1979 (Argüello et al. 2006).

The gully along which the studied profiles can be seen was formed by erosion due to extreme rainfall during the hydrological year 1978/1979, the soybean harvest coinciding with the rainy period that leaves the soil unprotected from erosion of the silt, accelerating the gully development, and also due to neotectonics, as shown by Kraemer et al. (1993) in the San Alberto Valley, and by Degiovanni and Cantú (1997) at the southern province. In simple terms, gullies develop when a channeling of the water flow disrupts the natural system and then causes retrograde erosion. The studied gully (locally called "cárcava") is known as Corralito after the town that is located not far away. The

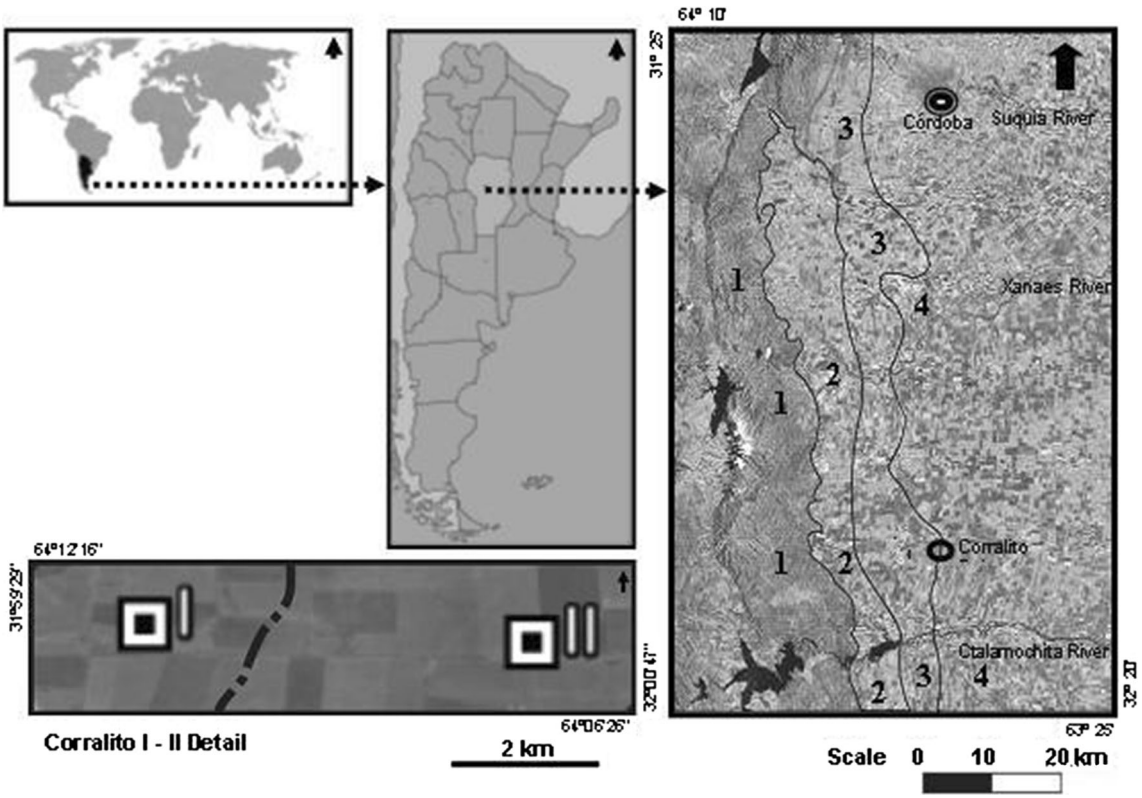

Fig. 1 Geomorphological map. *1* Córdoba ranges. *2* Peripheral depression. *3* Undulated tilted platform. *4* Flat tilted platform

total length of the gully is approximately 20 km, and its width varies between 20 and 40 m. The profiles are separated from each other by an approximate distance of 6 km, and their coordinates are: Corralito I, 32°0′7″ South; 64°11′8″ West, 469 masl (meters above sea level), and Corralito II: 32°0′16″ South; 64°7′21″ West, 433 masl.

Corralito I (Table 1) profile has a thickness of approximately 11 m and is constituted by a sequence of three paleosols intercalated with mantles of loess, and a buried soil on which recent anthropogenic sediments have accumulated (Frechen et al. 2009).

The luminescence studies carried out by Frechen et al. (2009) in the Corralito I profile established an age which corresponds to Late Pleistocene. The base of paleosol III was dated as 115 ± 21 ka and the youngest sediment is 13.8 ± 2.1 ka and corresponds to the buried soil. Paleosol I would, therefore, belong to MIS 3 and paleosol III to MIS 5 (Rouzaut et al. 2012). It should be noticed that paleosol III in both profiles has poor vertical development (Fig. 2), very likely because it has been partially eroded.

The anthropogenic landfill at the top of the profile was omitted from the sampling because it is not relevant to this study of magnetic properties as paleoclimate proxies. Instead, and to achieve a better interpretation and comparison of the analyzed parameters, it was replaced by the present natural soil. The samples of this soil are representative of the area, but because the zone is under intense agricultural use, they were taken from a small, untouched hill of pristine soil that lies a few kilometers away, in the same geomorphologic subassociation and belonging to the same soil series.

Profile Corralito II (Table 2) has a thickness of 21 m and consists of a sequence of three paleosols. Some fluvial deposits can be found at the base. Unlike Corralito I, this profile lacks a buried soil, since the current soil is exposed, although in use for agricultural purposes.

As Corralito I has already been dated by luminescence and some of its magnetic characteristics have already been analyzed (Rouzaut et al. 2012), it was selected as the main profile for establishing magnetic comparisons. Corralito II, as will be described below, has notable pedostratigraphic correlations with the regional pattern (Comité Argentino de Estratigrafía, CADE 1992).

Materials and methods

The profiles were measured, analyzed and described, and samples weighing 500 g were taken every 10 cm approximately. Care was taken to avoid the sampling of weathered material, krotovines and traces of roots to obtain the best possible resolution of the profile.

Particle size and calcium carbonate content were determined in bulk samples at vertical intervals of approximately 50 cm, using a laser diffraction particle analyzer (CILAS) and a Sheibler calcimeter (Gale and Hoare 1992), respectively. Both devices were available at the Geology Department of Buenos Aires University. Results were expressed as a mean for grain size and as a percentage for calcium carbonate content.

Representative samples of each horizon were chosen for the mineralogical analysis of sands. In the selected samples cements were destroyed and the material was dispersed by ultrasound. After sieving the samples, the fractions between 100 and 50 μm were studied. The mineralogical studies were carried out using polarized microscopy on a grain count of 1,000, following the method used by Karlsson (1990).

Before analyzing the magnetic properties, the samples were dried at room temperature, ground in a mortar and then placed in plastic containers for measurement and storage. All the samples were weighed to standardize the results.

The magnetic susceptibility measurements were performed at two frequencies (470–4,700 Hz) using a Bartington MS2. The hysteresis parameters were measured with a Vibrant (VSM) Molspin magnetometer with a maximum field of 1 Tesla. The parameters measured were magnetic susceptibility (X_{total}), saturation magnetization (M_s), saturation remanent magnetization (M_{rs}), coercivity (H_c) and remanent coercivity (H_{cr}).

During measurement, no cement of any kind was used since the sample holder of the magnetometer compacted the material and prevented the movement of particles.

Measurements of magnetic susceptibility at low and high temperatures were carried out on selected samples using an AGICO MFK1-FA Kappabridge with a frequency of 946 Hz and a field amplitude of 200 A/m. For measurements at high temperatures, the samples were gradually heated up to 700 °C while continuously monitoring X and then left to cool to room temperature. The entire process was performed in an Ar atmosphere to prevent mineral oxidation.

Measurements of magnetic susceptibility at low temperatures were carried out by cooling the samples to −200 °C and then measuring them until they reached room temperature.

The measurements of isothermal remanent magnetization were subjected to magnetic pulses of 300 and 1,000 mT in an ASC Scientific Pulse Magnetizer with coils that reach a field of 1.2 T. They were then measured in the AGICO JR-6 Dual Speed Spinner magnetometer. Using this data, the quotient IRM 300 mT/IRM 1,000 mT was established and the S-ratio was obtained.

Table 1 Paleopedological description of the Corralito I profile

Corralito I								
Horizon	Thickness (cm)	Color	Texture	Structure	pH	Coatings	Carbonates	Observations
Present soil								
A	20	Dry : 10 YR 4/2 Wet: 10 YR 3/2	Silty loam	Type: subangular blocky Class: medium to coarse Stability: moderate	6.5			
*B*w	15	D: 10 YR 4/4 W: 10 YR 3/3	Silty loam	Type: blocky Class: medium to coarse Stability: weak	6.5	Composition: clay humic and clay skin Abundance: poor Thickness: thin		
Loess								
BC	35	D: 10 YR 4/6 W: 10 YR 3/4	Silty loam	Type: blocky Class: medium Stability: weak	7			
Ck	10	D: 7.5 YR 5/6 W: 7.5 YR 4/4	Silty loam	Massive	>8		Plenty in the mass	
Buried soil								
Ab	10	D: 10 YR 3/3 W: 10 YR 2/3	Silty loam	Type: subangular blocky Class: medium to coarse Stability: moderate	6.5			
Btb	20	D: 7.5 YR 5/3 W: 10 YR 3/2	Silty loam	Type: prismatic and subangular blocky Class: medium to coarse Stability: moderate	6.5	Composition: Clayhumic (clhm) Abundance: abundant Thickness: medium		
Loess								
BCb	40	D: 7.5 YR 4/4 W: 7.5 YR 3/3	Silty loam	Type: subangular blocky Class: coarse Stability: weak	7	Composition: clhm Abundance: poor Thickness: thin		
Ckb	130	D: 7.5 YR 4/4 W: 7.5 YR 3/3	Silty loam	Massive	>8		Plenty in the mass Nodules >1 cm	32.7 ± 6.7 ka
Paleosol I								
2Btkb1	120	D: 5 YR 6/3 W: 2.5 YR 5/6	Silty loam	Type: irregular prisms Class: medium to coarse Stability: strong	>7	Composition: clhm Abundance: abundant Thickness: medium to thin		
2Btkb2	40	D:5 YR 7/4 W: 5 YR 5/6	Silt	Type: subangular blocky Class: medium to coarse Stability: moderate	>7	Composition: Clayskin (clsk) Abundance: abundant Thickness: medium		
Loess								

Table 1 continued

Corralito I								
Horizon	Thickness (cm)	Color	Texture	Structure	pH	Coatings	Carbonates	Observations
2BCkb1	30	D: 5 YR 7/4 W: 5 YR 5/6	Silt	Type: subangular blocky Class: moderate Stability: weak	>7		In the mass	Fragipans
2 Ckb1	50	D: 5 YR 7/4 W: 5 YR 6/6	Silt	Massive	>8		Nodules >1 cm	
Paleosol II								
3 Btkb3	60	D: 5 YR 8/4 W: 5 YR 4/8	Silt	Type: irregular prisms Class: medium to coarse Stability: strong	>7	Composition: clhm Abundance: Abundant Thickness: medium to fine	Moderate in the mass	Fragipans
3 Btkb4	130	D: 5 YR 8/4 W: 5 YR 5/6	Silty loam	Type: irregular prims Class: medium to coarse Stability: moderate	>7	Composition: clhm, clsk Abundance: Abundant Thickness: medium		Fragipans
Loess								
3BCkb2	30	D:5 YR 7/4 W: 5 YR 5/6	Loam	Type: subangular blocky Class: medium to coarse Stability: weak	>8		Moderado en masa	
3Ckb2	70	D: 5 YR 7/6 W: 5 YR 6/4	Loam	Massive	>8		Plenty in the mass Many nodules	66 ± 9.4 ka
Paleo. III								
4 Btkb5	40	D: 5YR 7/4 W: 5 YR 5/8	Silty loam	Type: irregular prisms. Class: moderate to coarse Stability: strong	>7	Composition: clsk Abundance: poor Thickness: thin		
Loess								
4 BCkb3	90	D: 5 YR 6/6 W: 5 YR 5/6	Silty loam	Type: subangular blocky Class: Moderate Grado: moderado-débil	>7			Fragipans
4 Ckb4	80	D: 5 YR 7/3 W: 5 YR 6/6	Loam	Massive	>8		Plenty in the mass Nodules >1 cm	115 ± 21 ka

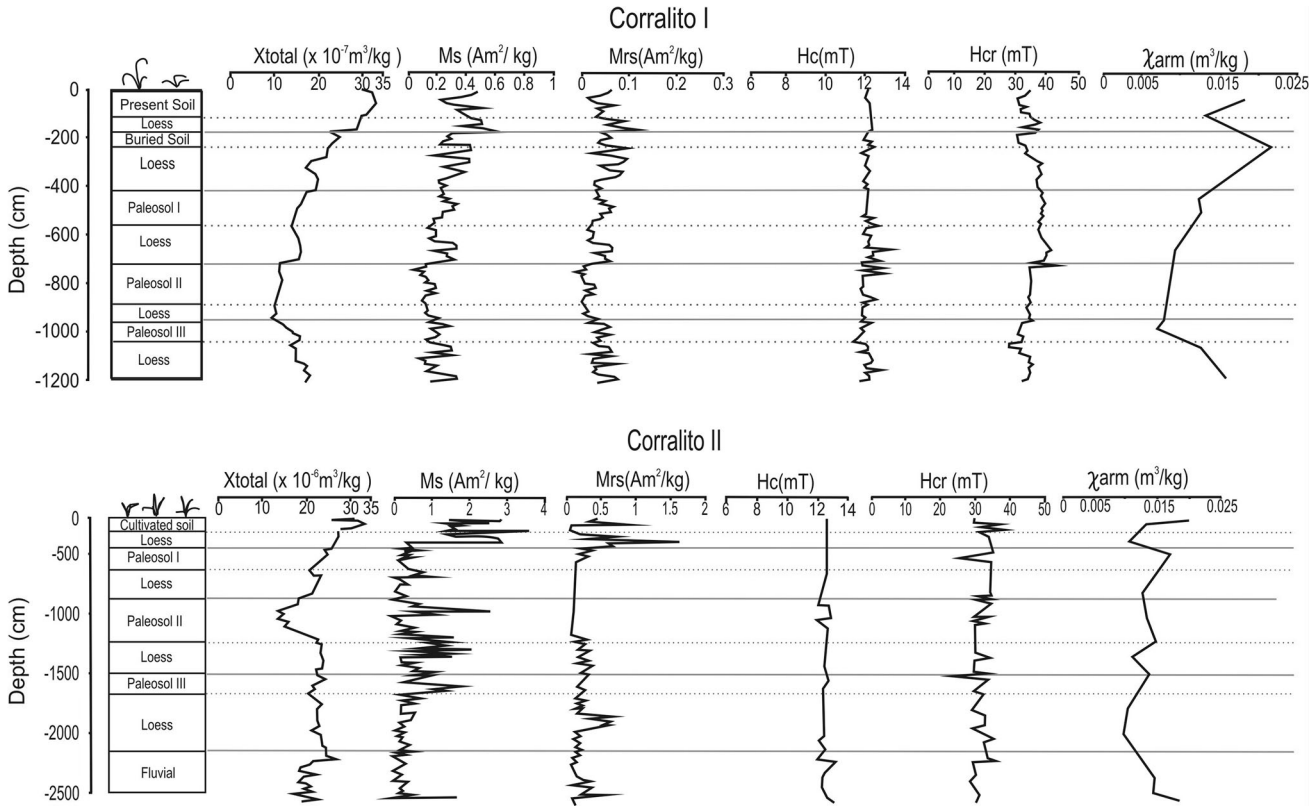

Fig. 2 Magnetic properties of Corralito I and Corralito II

Measurements of anhysteric remanent magnetization (ARM) were performed in selected samples of each profile and were carried out using the protocol proposed by Lisé-Pronovost et al. (2013). Following this procedure, selected samples were subjected to alternating fields of 100 mT and continuous fields of 0.05 mT in the AGIGO LDA-3 AF Demagnetizer with alternating, rotating field and anhysteretic magnetizer. These magnetizations were then measured in the AGICO JR-6 Dual Speed Spinner magnetometer. Table 3 summarizes the analyzed magnetic parameters and the information they suggest.

Results

Profiles

The Corralito I profile consists of a buried soil and three paleosols with intercalated loess layers (Table 1). The buried soil and paleosol horizons are mainly B_t, since they exhibit a strong prismatic structure and coatings with a high content of clay and organic matter. Melanization, decarbonatation–carbonatation and argilluviation are among the most noticeable pedogenetic processes. Underlying these horizons are the transitional BC horizons, which have been partially subjected to pedogenesis, and beyond them the C horizons in which the pedological processes have been more subtle. All these horizons are interrupted by lenses of 1 m in diameter of fragipan.

$CaCO_3$ is present in the profile, at close to 2 % in the buried soil and the paleosols, while the BC and C horizons—which shall be referred to as loess for simplicity—contain between 3 and 6 % overall.

The mean diameter of the particles ranges between 20 and 24 μm (medium silt) in the present-day soil, the buried soil and paleosols I, II and III. In the loess mantles, the average is within a range of 25–35 μm (medium to coarse silt).

Mineralogical studies on selected samples indicate that the dominant minerals are quartz, feldspar, volcanic glass, muscovite, biotite and in some cases hornblende. It is important to highlight the high percentage of volcanic glass (Fig. 3): 30 % in the buried soil, 20 % in paleosol I, 60 % in paleosol II and 40 % in paleosol III. The morphological classification of the glass was performed according to Karlsson and Ayala (2003).

The Corralito II profile (Table 2) includes the cultivated present-day soil, three paleosols with intercalated loess mantles of varying thickness, and finally fluvial sediment in the last 340 cm.

Table 2 Paleopedological description of the Corralito II profile

Corralito II								
Horizon	Thickness (cm)	Color	Texture	Structure	pH	Coatings	Carbonates	Observations
Cultivated soil								
Ap	30	Dry: 10 YR 5/2 Wet: 10 YR 2/1	Silty loam	Type: subangular blocky Class: thin Stability: weak	6.5			
Bw	40	D: 10 YR 5/3 W: 10 YR 4/4	Silty loam	Type: subangular blocky Class: medium Stability: moderate	6.5	Composition: Clayhumic (clhm) Abundance: poor Thickness: thin		Bioturbation
Loess								
BC	40	D: 7.5 YR 6/4 W: 7.5 YR 5/4	Silty loam	Type: subangular blocky Class: thin Stability: weak	7			
Ck	350	D: 7.5 YR 6/3 W: 7.5 YR 5/6	Silt	Massive	>8		Plenty in the mass	
Pal I								
Btkb	60	D: 7.5 YR 7/4 W: 7.5 YR 5/6	Silty loam	Type: irregular prisms Class: medium Stability: moderate to weak	>7	Composition: clsk Abundance: poor Thickness: thin		
Loess								
2Ckb	320	D: 5 YR 6/4 W: 5 YR 4/4	Silt	Massive	>8		Plenty in the mass Nodules >1 cm	
Pal II								
3Btkb	180	D: 7.5 YR 7/3 W: 7.5 YR 6/6	Silt	Type: irregular prisms Class: moderate Stability: strong	>8	Composition: clsk Abundance: abundant Thickness: thin		
Loess								
3Ckb2	260	D: 7.5 YR 7/4 W: 7.5 YR 6/8	Silt	Massive	>8		Many nodules	*Ctenomys?*
Pal III								
4Btkb3	50	D: 5 YR 6/3 W: 5 YR 5/4	Silt	Type: subangular blocky Class: moderate Stability: strong	>8	Composition: clsk Abundance: abundant Thickness: thin		
Loess								
4Ckb3	440	D: 7.5 YR 6/3 W: 7.5 YR 4/4	Silt	Massive	>8		Many nodules	
	340	Fluvial						

Table 3 Magnetic parameters and the information provided

Parameter	Interpretation[a]
Magnetic susceptibility (X mass specific units)	It is the contribution of ferrimagnetic minerals X_f, paramagnetic, X_p and diamagnetic X_d. Due to the low intrinsic magnetization of antiferromagnetic minerals, magnetic susceptibility is a measure of the concentration of ferrimagnetic minerals. It is dependent on the grain size and increases in the presence of SP and MD grains
Saturation magnetizaton (M_s); saturation remanent magnetization (M_{rs}), coercivity (H_c) and remanence coercivity (H_{cr})	M_s is the magnetization in the presence of a saturating field, M_{rs} is the remanent saturation which remains after removing the saturating field. These are extensive parameters which increase with grain size and concentration
	H_{cr} is the field required to rotate half the remanent magnetization to opposite direction from previous saturation, thus causing the remanent net magnetization to be zero. H_c is the field required to bring saturation magnetization to zero (from previous saturation, half the magnetic moments are rotated and the net moment would be zero). H_c and H_{cr} are useful parameters to identify mineralogy; low values indicate low coercivity minerals such as magnetite and titano-magnetite
Magnetic susceptibility as a function of temperature $X(T°)$	During warming, minerals lose their magnetic susceptibility (X) at specific temperatures which helps to identify minerals. Eg., 580 °C for pure magnetite, for hematite 670 °C. Crystallographic transitions are also important, because they occur at a certain temperature in some minerals. Eg., 120–258 K for magnetite and hematite
Susceptibility of anhysteretic remanent magnetization (χ_{arm})	ARM is the magnetization acquired under the presence of a direct field within a decreasing alternating field. The χ_{arm} is obtained by dividing the module obtained by the continuous field. Is particularly sensitive to grain sizes (SD and PSD). Increases with the concentration of magnetic particles
S-ratio	The procedure is to saturate a sample in the forward direction (SIRM) and then expose it to a backfield (typically equal to 0.3 T). The S-ratio is obtained by dividing the "backwards" remanence by the SIRM. This provides a fair estimate of the relative importance of antiferromagnetics (such as hard hematite) versus ferrimagnetics (such as soft magnetite)
Sizes SD, PSD, MD and SP	Magnetic minerals exhibit magnetic domains in which the magnetization is uniform but in different directions. They depend on the mineral composition For instance, for magnetite single domain grains SD: 0.1–0.05 μm; pseudo-single domain PSD: 1–0.1 μm, multidomain MD >1 μm. Superparamagnetic grains SP, <0.05 μm, do not present remanence at room temperature

[a] Verwey et al. (1947), Morin (1950), Dearing (1994), Hunt et al. (1995), Dunlop and Özdemir(1997), Egli and Lowrie (2002), Evans and Heller (2003), Lisé-Pronovost et al. (2013) (taken and modified from Vásquez-Castro et al. 2008)

Soil and paleosol are composed of a B_w and a B_t horizon, respectively. Both of them have clay coatings and subangular block structures. Below them, C horizons lie with abundant calcium concretions about 1 cm in diameter. Pedological processes are similar to those of the Corralito I profile, i.e., melanization, decarbonatation–carbonatation and argilluviation. There are no fragipans in this profile.

The lowest layer corresponds to 340 cm of fluvial sediments with a crisscross, charge-release structure that is covered with a 2 cm deep line of imbricated loess stones. The percentage of $CaCO_3$ is between 2 and 4 %, while mean grain size indicates medium to coarse silt (28–30 μm) throughout the whole profile.

The mineralogical analysis indicates the presence of minerals such as quartz, feldspar, muscovite, biotite and volcanic glass (Fig. 3). Same as in Corralito I, the percentage of volcanic glass is very high: 30 % in the cultivated present-day soil, 40 % in paleosol I and 50 % in paleosols II and III.

Magnetic results

The X_{total} of Corralito I (Fig. 2) decreases from the top of the present-day soil loess up to the base of the paleosol II, while in the paleosol III the trend reverses.

If the behavior of the buried soil and of each individual paleosol is examined, the following observations can be made.

The X_{total} shows no significant changes in paleosol III (decreasing slightly from 20 to 15 $\times$ 10^{-7} m^3/kg from bottom to top) or in paleosol II (increasing slightly from 10 to 15 $\times$ 10^{-7} m^3/kg from bottom to top). On the other hand, there is a very slight tendency towards an increase in the present natural soil, the buried soil and the paleosol I,

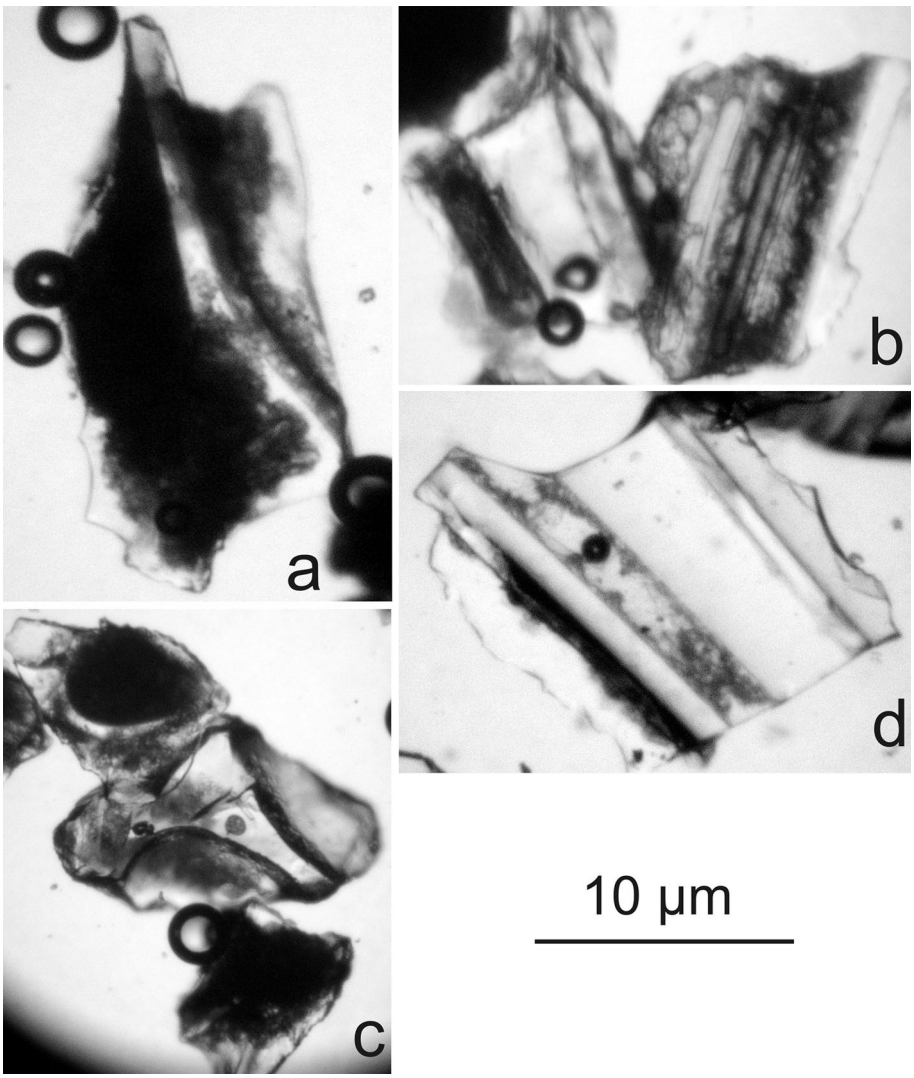

Fig. 3 Sorting glass pictures of the analyzed samples according to Karlsson and Ayala (2003). **a–c** Transparent fiber bundles with fluidal texture; **d** colorless triangular flat plates with fractures along microvacuoles

while loess does not have a similar trend. These fluctuations are accompanied by the extensive parameters M_s and M_{rs}, although M_s and M_{rs} show more variability and less range of variation (Max–Min).

H_c is steady between 12 and 14 mT, and the H_{cr} also shows no significant changes. In some ways, the χ_{arm} behaves similar to the X_{total}, in paleosol III there is a decrease from 0.015 to 0.01 m^3/kg and a small increase in paleosol I (0.01–0.011 m^3/kg) and paleosol II (0.009–0.01 m^3/kg), while in the present natural soil (0.015–0.02 m^3/kg) and the buried soil (0.011–0.015 m^3/kg) the increases are higher.

The *S*-ratio displays a value close to 0.9 throughout the whole profile, with the exception of two decreases (Fig. 4) at −200 and −420 cm where the *S*-ratio goes down to 0.8 and 0.6, respectively.

The variations in magnetic susceptibility at high temperatures (Fig. 5) for a loess sample indicate temperatures consistent with the Curie temperature for magnetite, hematite may also be present because significant kt still left above 580 °C. Increases in the heating curves may be associated with the formation of magnetite in an anoxic environment during the heating. Variations in magnetic susceptibility at low temperatures of the Corralito I loess sample (Fig. 5) show a high concentration of fine-grained particles of magnetite (or maghemite) at the SP–SD limit.

The magnetic particle size for Corralito I (Fig. 6a), as shown by the M_{rs}/M_s and H_{cr}/H_c ratios (Dunlop 2002), indicates a pseudo-single domain (PSD) with some superparamagnetic particles (SP) and some of the data points plot closer to the SD–MD mixing line which means a significant contribution of MD particles in some of the Corralito I profile sections.

The X_{total} signal in Corralito II (Fig. 2) shows a decreasing trend from the top down to −1,000 cm of the profile while from −1,000 to −2,200 cm it remains virtually unchanged and fluctuates again in the fluvial sediments at the base of the profile.

The X_{total} in paleosol III shows a negligible increase (from 20 to 21 $\times$ 10^{-6} m^3/kg), in paleosol II it shows a significant decrease from 25 to 10 $\times$ 10^{-6} m^3/kg; in paleosol I there is a slight increase towards the top. Finally, there is a noticeable increase in X_{total} with respect to the parental material in cultivated present-day soil from 28 to 35 $\times$ 10^{-6} m^3/kg, (Fig. 2).

Extensive properties (Fig. 2), such as M_s and M_{rs}, do not accompany the trends described for the X_{total}; instead, these parameters are highly variable throughout the profile.

Hc is always between 12 and 13 mT, while H_{cr} is similar to that of Corralito I with almost irrelevant variations. The χ_{arm} could have a similar trend to the X_{total}, although this is not entirely clear. The χ_{arm} observed increases in paleosol III (0.010–0.015 m^3/kg), paleosol I (0.013–0.015 m^3/kg) and in the cultivated present-day soil (0.01–0.02 m^3/kg). On the contrary, in paleosol II the value decreases from 0.015 to 0.01 m^3/kg.

The *S*-ratio is steady at 0.9 (Fig. 4) down to paleosol II, where there is a significant decrease, reaching values as low as 0.2; this values are surprisingly low, but not very high H_{cr} values are observed. There is not any clear explanation for these results. Perhaps, in this case the mixture of magnetic minerals and grain size is such that the coercivity values are further controlled by ferrimagnetic fraction. At the base of the profile, the *S*-ratio ranges between 0.6 and 0.9.

Variations of magnetic susceptibility at high temperatures (Fig. 5) for a loess sample are consistent with magnetite. As in Corralito I, increases in the heating curves may be associated with magnetite formation during heating. The variations of magnetic susceptibility at low temperatures of the Corralito II loess sample show a remarkable Verwey transition consistent with the presence of multidomain (MD) magnetite.

The size of the magnetic particles in Corralito II (Fig. 6b; Dunlop 2002) indicates a PSD with mixtures of single domain–multidomain (SD–MD) and single domain–superparamagnetic (SD–SP).

Discussion

The different thickness of Corralito I and Corralito II profiles, with 11 and 21 m, respectively, is due to the different geomorphological position of both profiles. Corralito I lies in the undulated tilted platform, at an interfluve where water concentrates and infiltrates. Instead, Corralito II is in the flat tilted platform where the lower slope causes water to drain as sheet flow. Therefore, the infiltration is lower and consequently is the paleosols thickness as well. Additionally, different slopes generate differential erosion that is reflected in the geological record. Both profiles are nowadays subjected to the same climatic regime and, therefore, it is assumed that they also were in the past. Consequently pedogenetic processes are similar in both profiles. Pedogenetic processes affecting both profiles are: melanization, decarbonatation–carbonatation and argilluviation. Fragipans were developed only in Corralito I. The process of melanization (from the Greek word *Mélas* = black) is the modification of chemical and biochemical material leading to darkening due to the incorporation of organic residues from plant and animal compounds. This process is easily recognized, just by looking at the color variation with respect to the lower horizons.

In the case of the paleosol, horizon A is assumed to have been eroded, but in case it has not, it is difficult to identify, because its carbon content has most likely been depleted as a result of diagenesis (Imbellone et al. 2010). This is a quick process that requires the presence of flora and fauna in the soil to partially decompose the organic materials in the soil and produce instead stable dark compounds which are then mixed up by various organisms (earthworms, ants, rodents). Mild weather and proper moisture conditions are needed for biota to be present.

The percentage of $CaCO_3$ is low for both profiles, and on average it does not exceed 5 %. Although it can be found throughout the whole profile, the presence of $CaCO_3$ in the paleosols is the result of the removal of carbonates from the overlying loess mantles. This can be seen in the field when taking a sample from a B_t horizon of any of the paleosols and testing it with HCl 1 N. The resulting reaction only takes place on the outside and not in the center of the aggregate. The presence of calcium carbonate throughout the profiles is the result of a process known as decarbonatation–carbonatation. Decarbonatation is the result of the movement of carbonates which dissolve in the form of soluble bicarbonate and then move with seepage water. Conversely, carbonatation occurs when bicarbonates turn into insoluble carbonates again and are then deposited. Calcium carbonate precipitates when CO_2 pressure decreases as a result of a decrease in biological activity (porosity decreases with depth and thus the availability of oxygen, essential for respiration of organisms, is much lower). Carbonates can have an eolian origin, as is the case of the studied area (Dorronsoro and Aguilar 1988). However, regardless of the origin, in the final phase of the accumulation of carbonates, the hydrological conditions of the profile play a decisive role (Dorronsoro and Aguilar 1988). Both dissolution and precipitation require the presence of water in the profile, therefore, it is assumed that the climate is humid.

The presence of fragipan sectors in Corralito I also indicates humid climatic conditions. They are horizons densified and brittle by hydrocompaction and ligand agents (clay bridges, silica, aluminum and organic matter).

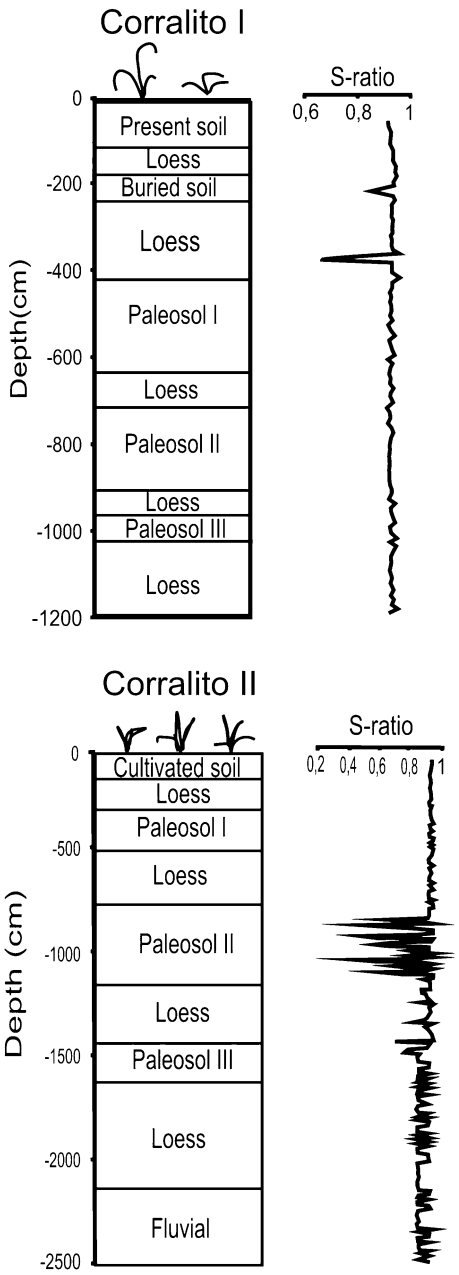

Fig. 4 *S*-ratio, magnetic mineralogy indicator

Imbellone et al. (2005, 2010) found fragipans in Argentine polycyclic soils, probably resulting from auto-compaction and acid hydrolysis, as in the case of the province of Córdoba (Schiavo et al. 1995).

The material removed from the upper horizons probably accumulated in the B_t and B_w horizons through the process of argilluviation (Dorronsoro and Aguilar 1988), which consists of the mechanical transportation of clay and/or organic matter particles. These particles are washed and coated during the movement caused by rain water. Coatings are clearly visible in the B_t horizons and barely perceptible in the B_w. This process requires a climate with contrasting seasons, as found in the studied area at present.

The analysis of particle size in both profiles showed similar results (medium to coarse silt). However, these fractions fluctuate considerably throughout the profiles, which could indicate that there was some reworking after the initial deposition, as suggested by Argüello et al. (2012) after studying the soils in the area.

In the mineralogical analysis, it can be seen that volcanic glass content (amorphous silica) is very high (between 30 and 60 %), particularly in the paleosol II of both profiles. These high percentages of dissolved or amorphous silica can generate the dissolution of detrital ferrimagnetic minerals under any redox and pH conditions (Florindo et al. 2003), which can interfere with paleoclimatic interpretations obtained through magnetic parameters (Orgeira et al. 2011).

The X_{total} of Corralito I is markedly lower with respect to Corralito II, thus suggesting that Corralito II has a higher concentration of ferrimagnetic minerals. The difference in the concentration of magnetic minerals between both sections could be related to their different geomorphological positions. The Corralito I profile is located on low land, on a runoff line and with moderate drainage, thus allowing the development of thick soils which retain a greater amount of water after rainfall; excess water is removed, but rather slowly. The drainage is determined by conditions related to slope, runoff, permeability and phreatic bed depth (Etchevehere 1976). Consequently the whole profile quite often undergoes reductive conditions, which could generate appropriate and relatively permanent conditions for the loss of magnetic minerals. On the other hand, the Corralito II profile has consistently better drainage, which mainly generates oxidative conditions and water infiltration rather than water accumulation as in Corralito I. Minimal but continuous syn-sedimentary pedogenesis would also occur.

In the two studied profiles, there seems to be a similar tendency of the χ_{arm} and the X_{total}, which is expected due to the proximity of the profiles. In both profiles, from the two paleosols II and upwards, the trend towards a progressive increase in the extensive magnetic parameters X_{total}, partially accompanied by M_s and M_{rs}, is indicative of an increase in the concentration of magnetic minerals.

Minor M_s and M_{rs} fluctuations, as well as oscillations in the grain size determined by particle size analysis, are indicators of slight changes in the particle size due to water remobilization (by resuspension and redeposition) after the primary wind deposition (Argüello et al. 2012).

An *S*-ratio close to 1 throughout the Corralito I profile (Fig. 4) indicates the presence of a mineral with a low coercivity such as magnetite; these results are consistent with the H_c and H_{cr} arising from the hysteresis cycle, as well as with susceptibility changes at high temperatures.

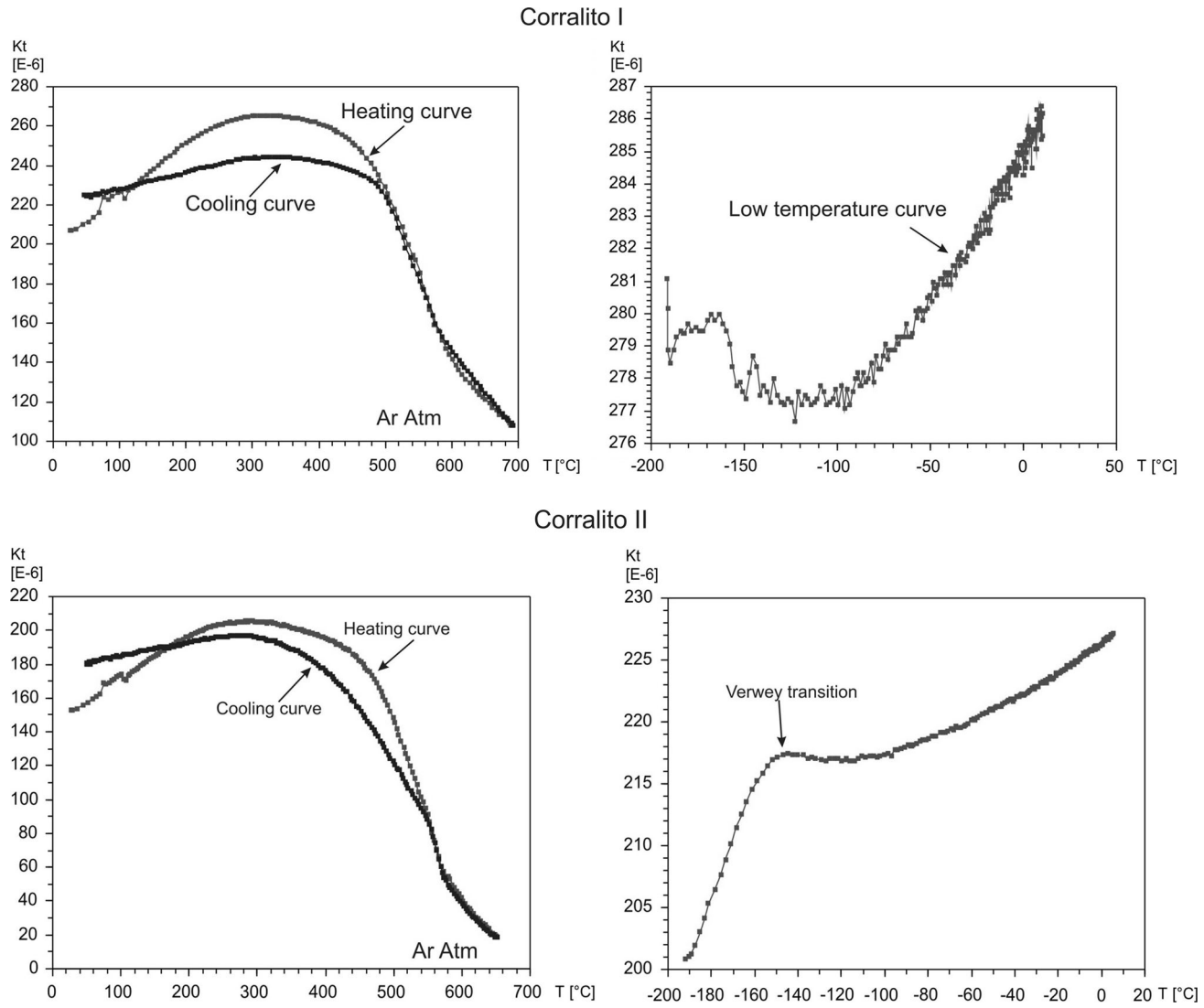

Fig. 5 High and low temperatures, representative of the profiles Corralito I and Corralito II

Only two layers at −200 and −420 cm have lower ratios (0.8 and 0.6, respectively). Both pedogenized levels (the buried soil and the bottom of loess of the mentioned soil) show evidence (*S*-ratio, magnetic susceptibility at high temperature and the profile color, see Table 1) of minerals with high coercivity such as hematite, which suggests oxidation during the pedogenesis. As it was mentioned in previous paragraphs, lower values of *S*-ratio are not associated with H_{cr} high values. We do not have a clear explanation for these results. Perhaps, the mixture of magnetic minerals and grain size is such that the H_{cr} values are further controlled by ferrimagnetic fraction.

An *S*-ratio close to 1 throughout the Corralito II profile (Fig. 4) also indicates magnetite, consistent with the coercivity values. However, paleosol II shows variations down to values close to 0.2. These values clearly demonstrate the abundance of high coercivity minerals such as hematite, associated with strong oxidative processes during pedogenesis. This oxidation could correspond to a period with dryer seasons. On the other hand, both profiles are inside a gully which implies retrograde erosion and, therefore, Corralito II was exposed and its magnetic minerals are oxidized (hematite) as shown by *S*-ratio, mainly at paleosol II.

The results of variations in susceptibility at low temperatures obtained in loess samples from Corralito I and Corralito II (Fig. 5) indicate grain sizes similar to those reported by the comparison between Dunlop (2002) ratios (Fig. 6a, b). For the Corralito I loess sample, SP magnetite particles are progressively unlocked as the temperature increases (at low temperatures they behave like SD), which would also be consistent with the presence of paramagnetic minerals highlighted by the high susceptibility values. In the Corralito II loess sample, the Verwey transition points

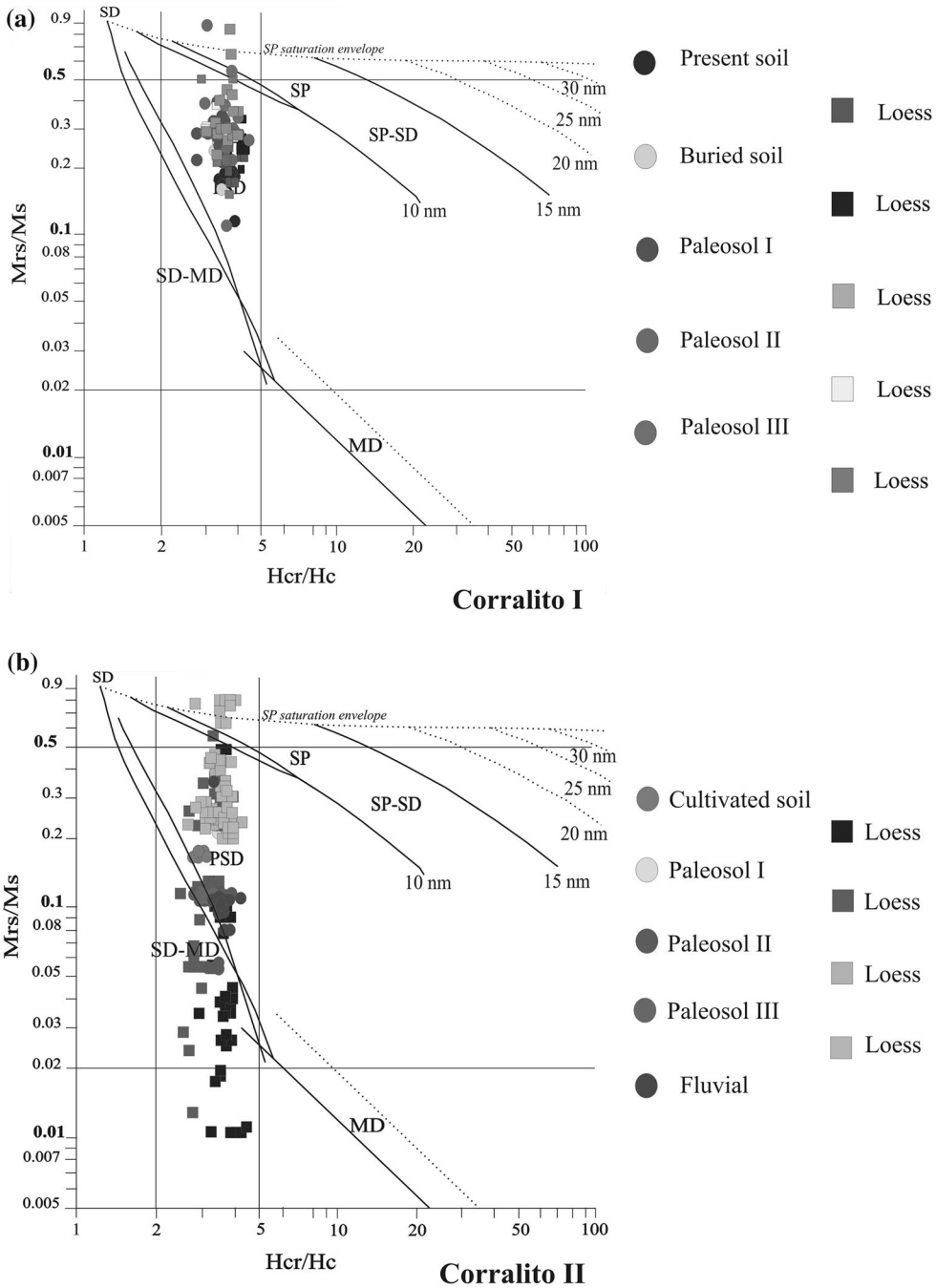

Fig. 6 **a** Magnetic minerals domain state in Corralito I, according to Dunlop (2002). **b** Magnetic minerals domain state in Corralito II, according to Dunlop (2002)

to MD magnetite and perhaps some SP size minerals, which are indicated by the increase in susceptibility with temperature (Fig. 5).

According to the hysteresis parameters that were obtained the size of magnetic particles in both profiles is generally PSD (Fig. 6a, b). In Corralito II the mixture of PSD, SD and MD sizes is more noticeable, which reinforces the idea of sediment reworking. It is interesting to note that the loess levels contain SP particles (Fig. 6b); these SP particles might correspond to inclusions of magnetite in unaltered volcanic glass.

Although magnetic results are not exactly the same (there are different concentrations of magnetic minerals, slight differences in H_{cr}), the magnetic behavior (an increase in concentration of magnetic particles) of the present soil and paleosol I in Corralito I and present cultivated soil and paleosol I in Corralito II is similar. Considering the hypothesis proposed by Orgeira et al. (2011), according to our interpretation, it would indicate climatic conditions similar to the present-day ones or similar conditions of water storage during pedogenesis. This is a qualitative argument. It is not possible at present to make a

quantitative estimation of water balance, since an efficient way to quantify the effect of some geological variables mentioned by Orgeira et al. (2011), such as the volcanic glass content, has not yet been developed.

It should also be noticed that the remarkable increase in the magnetic signal of the cultivated present-day soil in Corralito II may be due to the contribution of fertilizers. One of the most commonly used in the area is monocalcium phosphate, $Ca(H_2PO_4)_2{\cdot}2H_2O$, which includes many iron-rich impurities (Rouzaut et al. in preparation).

The decrease in the concentration of magnetic particles in paleosol II, which is notable at Corralito II and moderate at Corralito I, could indicate more humid and seasonally contrasting conditions during pedogenesis compared with today. This loss of ferrimagnetic particles could also be due to the presence of silica-rich fluids during pedogenesis. It should be noted that paleosol II has the highest percentage of volcanic glass in both profiles (50 and 60 %) On the other hand, the loss of ferrimagnetic minerals (detrital magnetite), is associated with the generation of pedogenic hematite during the dry seasons, which is clearly detected by the *S*-ratio at Corralito II, where the profile is better drained and exhibits more oxidative conditions. As mentioned above, paleosol I is assigned to MIS 3 and paleosol III to MIS 5. However, paleosol III in both profiles is very thin (Fig. 2), probably because it is partially eroded. Magnetic results indicate that during MIS 3 climatic conditions might have been similar to the present-day ones. MIS 5, poorly represented in the geological record of the area, does not present obvious magnetic properties which enable paleoclimatic assessments.

After comparing these results with others obtained in the country on profiles partially comparable in age, it is clear that the magnetic signals differ. Research work conducted by Orgeira et al. (2001, 2002, 2003) in Lujan shows sample results pertaining to Puesto Callejón Viejo soil, outcropping at the top of Guerrero Member of Luján Formation (minimum age ranging between 13,000 and 29,000 years). The same paleosol was also studied by Walther et al. (2004) in San Antonio de Areco. The beginning of this paleosol genesis was attributed by various authors to MIS 3.

All those researches detected an impoverishment of detrital magnetite during edaphic process. Simultaneously antiferromagnetic minerals assignable to hematite and/or goethite and ultrafine magnetite (SP) of pedogenic origin would have been generated. Bidegain et al. (2001) arrived at similar conclusions in loess sediments in the quarry Gorina, La Plata, attributing the results to dissolution of detrital magnetite as a result of weathering phenomena.

The above-mentioned results correspond to materials temporarily comparable to the buried soils of Corralito I. In this case the magnetic signal showed a slight increase of magnetic minerals at Corralito I.

The hypothesis developed by Orgeira and Compagnucci (2006) and Orgeira et al. (2011) suggests that the processes of alteration of the magnetic mineralogy during pedogenesis are not linear. It also proposes the existence of paleoclimatic thresholds. The study area of Córdoba would be close to one of those thresholds. At this area, according to the above-mentioned hypothesis, neither significant generation, nor total loss of ferrimagnetic minerals would be expected. The amount of magnetic minerals would be nearly balanced with respect to pre-pedogenesis initial state. The annual *W* index (comparable to the water balance of the soil) for Corralito I and Corralito II is −10.35. This means that according to climatological data the area at present exhibits a small, negative annual water balance. Then, the hypothesis for this area suggests a slight increase in the magnetic signal associated with the generation of small amounts of magnetite and preservation of detrital magnetite and titano-magnetite. The results in this paper show a slight gain in the buried soils of Córdoba that would confirm the hypothesis.

Conclusion

All the measured parameters indicate a high correlation between the profiles. However, the thickness of paleosols in Corralito I and Corralito II is variable, which could be a result of variable degrees of preservation (erosion differences) or of their location inside different geomorphologic subassociations. Pedological processes that took place in the paleosols indicate seasonally contrasting climates which allowed the preservation of magnetite, even with high percentages of volcanic glass. However, the results obtained in the Corralito II paleosol II show a remarkable loss of detrital ferromagnetic minerals associated to the neoformation of pedogenetic minerals with a high coercivity. This may be the result of a seasonally more humid climate with a very contrasting dry season.

Paleosol I is assigned to MIS 3 and paleosol III to MIS 5. Paleosol III in both profiles is very thin, and may be partially eroded. Magnetic results might indicate that MIS 3 in the area was similar to the current climatic conditions; MIS 5, poorly represented here in the geological record, does not present conspicuous magnetic properties that enable paleoclimatic assessments.

Acknowledgments This work was funded by projects Agencia PICT 0382/07 and PIP 747/10. Geologist Pablo Eveling's collaboration in the field work was vital to obtaining the present results. We also would like to thank to the anonymous referees for their suggestions which help us to improve our paper.

References

Argüello GL, Dasso CM, Sanabria JA (2006) Effects of intense rainfalls and their recurrence: case study in Corralito ravine, Córdoba Province, Argentina. Q Int 158:140–146

Argüello GL, Dohrmann R, Mansilla L (2012) Loess of Córdoba (Argentine) Central Plain, present state of knowledge and new results of research. In: Rossi AE, Miranda LS (eds) Capitulo en el libro Argentina: Educational, Geographical and Cultural Issues. Nova Science Pub Incorporated, New York, pp 1–49

Banerjee SK, Hunt C (1993) Separation of local signals from the regional paleomonsoon record of the Chinese loess plateau: a rock-magnetic approach. Geophys Res Lett 20(9):843–846

Bidegain JC, van Velzen AJ, Rico Y (2001) Parámetros magnéticos en una secuencia de loess y paleosuelos del Cenozoico tardío en la cantera de Gorina, La Plata: su relevancia en el estudio de los cambios paleoclimáticos y paleoambientales. Revista de la Asociación Geológica Argentina 56(4):503–516

Bidegain JC, Evans ME, van Velzen AJ (2005) A magnetoclimatological investigation of Pampean loess, Argentina. Geophys J Inter 160:55–62

Bloom A (1990) Some questions about the Pampean loess. In: Zárate M (ed) Properties, chronology and paleoclimatic significance of loess. International Symposium on Loess, Mar del Plata, pp 29–31

Boyle J, Dearing J, Blundell A, Hannam J (2010) Testing competing hypotheses for soil magnetic susceptibility using a new chemical kinetic model. Geology 38(12):1059–1062

Capitanelli R (1979) Geomorfología. In: Vázquez JB (ed) Geografía Física de Córdoba. Editorial Boldt, Buenos Aires, pp 213–296

Clapperton C (1993) Quaternary geology and geomorphology of South America. Elsevier, Scotland

Comité Argentino de Estratigrafía (CADE) (1992) Código Argentino de Estratigrafía. Asociación Geológica Argentina, Serie B, Didáctica y Complementaria 20:1–64

Dearing JA (1994) Environmental magnetic susceptibility. Using the Bartington MS2 system. Chi Publishing, England

Degiovanni S, Cantú M (1997) Neotectonic activity in the La Cruz-Gigena depression, Córdoba, Argentina. Suplementi di Geografi y Física e Dinamica Quaternaria. Fourth International conference on Geomorphology. Bologna III 1:142–143

Dorronsoro C, Aguilar J (1988) El proceso de iluviación de arcilla. Anales de Edafología y Agrobiología XLVII:310–350

Dunlop DJ (2002) Theory and application of the Day plot (Mrs/Ms versus Hcr/Hc). Theoretical curves and tests using titanomagnetite data. J Geophys Res 107(B3):1029–2001

Dunlop D, Özdemir Ö (1997) Rock magnetism: fundamentals and frontiers. Cambridge University Press, Cambridge

Egli R, Lowrie W (2002) Anhysteretic remanent magnetization of fine magnetic particles. J Geophys Res 107:10–21

Etchevehere P (1976) Normas de Reconocimiento de Suelos. INTA. Departamento de Suelos. Public. (152), Castelar, Buenos Aires

Evans ME, Heller F (2003) Environmental magnetism, principles and applications of enviromagnetics. Academic Press, San Diego

Florindo F, Roberts AP, Palmer M (2003) Magnetite dissolution in siliceous sediments. Geochem Geophys Geosyst. doi:10.1029/2003GC000516

Frechen M, Seifert B, Sanabria JA, Argüello GL (2009) Chronology of Late Pleistocene pampa loess from the Córdoba area in Argentina. J Q Sci Rev 23:1–12

Frenguelli J (1955) Loess y limos pampeanos. Serie Técnica y Didáctica No 7. Reimpresión. Universidad Nacional de La Plata, La Plata

Gale SJ, Hoare PG (1992) Quaternary sediments: petrographic methods for the study of unlithified rocks. Belhaven Press, London

Heller F, Evans ME (1995) Loess magnetism. Rev Geophys 33:211–240

Heller F, Shen CD, Beer J (1993) Quantitative estimates of pedogenic ferromagnetic mineral formation in Chinese loess and paleoclimatic implications. Earth Planet Sci Lett 114:385–390

Hunt C, Moskowitz B, Banerjee S (1995) Magnetic properties of rocks and minerals. In: Ahrens TJ (ed) Rock physics and phase relations: a handbook of physical constants, vol 3. American Geophysical Union, Washington, DC, pp 189–204

Imbellone PA, Giménez JE, Cumba A (2005) Suelos con "fragipán" de la Pampa arenosa. Actas XVI Congreso Geológico Argentino, pp 65–72

Imbellone PA, Giménez JE, Panigatti JL (2010) Suelos de la Región Pampeana: Procesos de formación. Ed. INTA

Iriondo M (1990) The upper Holocene dry climate in the Argentine plains Quaternary of South America, vol 7. Balkena Publ., Rotterdam

Iriondo M (1997) Models of deposition of loess and loessoids in the upper Quaternary of South America. J S Am Earth Sci 10(1):71–79

Iriondo M, Kröhling D (1995) El Sistema Eólico Pampeano 5(1):1–68

Karlsson A (1990) Aspectos del material piroclástico de los loess de Córdoba, Argentina. Actas del XI Congreso Geológico Argentino, Tomo I:434–438

Karlsson A, Ayala R (2003) Tipificación mineralógica de tefras asociadas a diferentes sedimentos cuaternarios. Cuaternario y Geomorfología. Editorial Magna Publicaciones, pp 111–119

Kemp JA, Zárate M, Toms P, King M, Sanabria JA, Argüello GL (2006) Late Quaternary paleosols, stratigraphy and landscape evolution in the Northern Pampas, Argentina. Q Res 66:119–132

Kraemer P, Tauber A, Schmidt T, Rame G (1993) Análisis cinemático de la falla de Nono. Evidencia de actividad neotectónica. Valle de San Alberto, Pcia de Córdoba. Actas del 12° Congreso Geológico Argentino y 2° Congreso de Exploración de Hidrocarburos Mendoza 3:277–281

Lisé-Pronovost A, St-Onge G, Gogorza C, Haberzettl T, Preda M, Kliem P, Francus P, Zolitschka B (2013) High-resolution paleomagnetic secular variation and relative paleointensity since the Late Pleistocene in Southern South America. Q Sci Rev 71:91–108

Liu X, Rolph T, Bloemendal J, Shaw J, Liu TS (1995) Quantitative estimates of paleoprecipitation at Xinfeng, in the Loess Plateau of China. Palaeogeogr Palaeoclimatol Palaeoecol 13:243–248

Maher BA (1998) Magnetic properties of modern soils and Quaternary loessic paleosols: paleoclimatic implications. Palaeogeogr Palaeoclimatol Palaeoecol 137:25–54

Maher BA, Thompson R (1995) Paleorainfall reconstructions from pedogenic magnetic susceptibility variations in the Chinese loess and paleosols. Q Res 44:383–391

Morin FJ (1950) Magnetic susceptibility of α-Fe2O3 and α-Fe2O3 with added titanium. J Phys 3:819–820

Muhs DR, Zárate M (2001) Late Quaternary eolian records of the Americas and their paleoclimatic significance. In: Markgraf V (ed) Interhemispheric climate linkages. Academic press, San Diego

Oches E, Banerjee S (1996) Rock-magnetic proxies of climate change from loess–paleosol sediments of the Czech Republic. Stud Geophys Geod 40:287–300

Orgeira MJ, Compagnucci R (2006) Correlation between paleosol-soil magnetic signal and climate. Earth Planets Space, Special Issue "Paleomagnetism and Tectonics in Latinamerica" 58(10):1373–1380

Orgeira MJ, Compagnucci RH (2010) Uso de la señal magnética de suelos y paleosuelos como función climática. Revista de la Asociación Geológica Argentina 65(4):612–623

Orgeira MJ, Walther AM, Vasquez CA, Di Tommaso I, Alonso S, Sherwood G, Yuang Hu, Vilas JFA (1998) Mineral magnetic record of paleoclimate variation in loess and paleosol from the Buenos Aires formation (Buenos Aires, Argentina). J S Am Earth Sci 11(6):561–570

Orgeira MJ, Walther AM, Tófalo R, Vásquez CA, Lippai HF, Compagnucci R (2001) Estratigrafía y magnetismo de rocas en un perfil del arroyo Tapalqué, Cuaternario de la provincia de Buenos Aires: implicancias paleoambientales y paleoclimáticas. Revista de la Asociación Geológica Argentina 56(3):353–366

Orgeira MJ, Walther AM, Tófalo R, Vásquez C, Berquó T, Favier Dubois C, Böhnel H (2002) Magnetismo ambiental en un paleosuelo desarrollado en la Fm Luján (Luján, Pcia. De Buenos Aires); consideraciones paleoclimáticas. Revista de la Asociación Geológica Argentina 57(4):451–462

Orgeira MJ, Walther AM, Tófalo R, Vásquez CA, Berquó T, Favier Dubois C, Bhonel H (2003) Environmental magnetism in paleosoils developed in fluvial and loessic Holocene sediments from Chacopampean Plain (Argentina). J S Am Earth Sci 16:259–274

Orgeira MJ, Egli R, Compagnucci R (2011) A quantitative model of magnetic enhancement in loessic soils. In: (IAGA special Sopron book series) Earth magnetic interior, vol 25. Springer, pp 361–368

Porta Casanellas J, Lopez-Acevedo Reguerin M, Roquero de Laburu C (2003) Edafología para la agricultura y el ambiente. Ediciones Mundi-Prensa, Madrid

Rouzaut S, Orgeira MJ, Vásquez C, Argüello GL, Sanabria J (2012) Magnetic properties in a loess–paleosol sequence of Córdoba, Argentina. Revista de la Sociedad Geológica de España 25(1–2):55–63

Rouzaut S, Orgeira MJ, Bachmeier O. Propiedades magnéticas en suelos cultivados (in preparation)

Sanabria J, Argüello GL, Moretti L (2006) Implicancia Paleoambiental de los paleosuelos de un sector de la Llanura Pampeana de Córdoba. Argentina, resumen publicado en el Taller de Cuaternario del XX Congreso Argentino de la Ciencia del Suelo, Salta

Schiavo HF, Becker AR, Cantú, MP (1995) Caracterización y génesis de los fragipanes de la depresión Curapaligüe. Dpto. Sáenz Peña, Córdoba. Argentina. Suplemento IDIA 33:659–673

Teruggi ME (1957) The nature and origin of the Argentinean loess. J Sediment Petrol 27:322–332

Vásquez-Castro G, Ortega-Guerrero B, Rodríguez M, García S (2008) Mineralogía magnética como indicador de sequía en los sedimentos lacustres de los últimos 2600 años de Santa María de Oro, México. Revista Mexicana de Ciencias Geológicas 25(1):21–38

Verwey EJ, Haayman PW, Romeijn FC (1947) Physical properties and cation arrangements of oxides with spinel structure. J Chem Phys 15:181–187

Walther AM, Orgeira MJ, Lippai HF (2004) Magnetismo de rocas en sedimentos cenozoicos tardíos en San Antonio de Areco provincia de Buenos Aires. Revista de la Asociación Geológica Argentina 59(3):433–442

Zárate MA (2003) Loess of southern South America. Q Sci Rev 2:1987–2006

Zárate M, Blasi A (1993) Late Pleistocene–Holocene eolian deposits of the southern Buenos Aires province, Argentina: a preliminary model. Q Int 17:15–20

Zárate M, Tripaldi A (2011) The aeolian system of central Argentina. Aeolian Res 3(4):401–417